

Supramolecular Chemistry | Hot Paper |

Mutually Exclusive Cellular Uptake of Combinatorial Supramolecular Copolymers

Sam van Dun, Jurgen Schill, Lech-Gustav Milroy, and Luc Brunsveld*^[a]

Abstract: The cellular uptake of self-assembled biological and synthetic matter results from their multicomponent properties. However, the interplay of the building block composition of self-assembled materials and uptake mechanisms urgently requires addressing. It is shown here that supramolecular polymers that self-assemble in aqueous media, are a modular and controllable platform to modulate cellular delivery by the introduction of small ligands or cationic moieties, with concomitantly different cellular uptake

kinetics and valence dependence. A library of supramolecular copolymers revealed stringent mutually exclusive uptake behavior in which either of the uptake pathways dominated, with sharp compositional transition. Supramolecular biomaterial engineering thus provides for adaptive platforms with great potential for efficient tuning of multivalent and multicomponent systems interfacing with biological matter.

Introduction

The assembly of supramolecular polymers relies more on non-covalent interactions than in covalent polymers, which leads to material properties unique to supramolecular polymers.^[1–3] Noncovalent interactions introduce reversibility, which makes supramolecular polymers more dynamic, responsive to external stimuli and fit for the bottom-up generation of libraries of multivalent polymers with high precision and complexity.^[4,5] Inspired by nature, in which supramolecular assemblies such as exosomes and viruses are involved in the intracellular delivery of cargo molecules, synthetic supramolecular assemblies have been successfully used as cellular delivery platforms.^[6] Besides the well-known liposomes,^[7] a broad range of functional supramolecular materials has been developed of which size, shape, stability, and valency can be controlled.^[6,8–10] The manner of dual targeting with which supramolecular polymers interact with the cellular membrane has been shown to depend on their valency and chemical composition.^[11,12] Driven by electrostatic interactions with anionic cell-surface proteoglycans, the introduction of cationic residues can initiate crossing of the

membrane, which is controlled by the density and distribution of charges.^[13–18] Also for alternative morphologies such as one-dimensional supramolecular polymers, cellular uptake could be induced via different intracellular trafficking pathways dependent on the monomeric building blocks.^[19,20] Similarly, ligands such as the small arginine-glycine-aspartic acid peptide (RGD) demonstrated an increased affinity for $\alpha v \beta 3$ integrin expressing cells when presented in a multivalent manner.^[21,22] The adaptability of a supramolecular polyrotaxane polymer, featuring RGD ligands, enhanced contact with integrin on the cellular membrane.^[23] Despite the examples of supramolecular materials interfacing with cellular surfaces,^[3,9,12] the influence of the composition of the supramolecular (co-)polymer on cellular uptake is still poorly studied. Supramolecular assemblies with a combination of targeting ligands and charges have demonstrated their advantages for in vitro studies^[24] but typically focused on single compositions, and lack comparison of copolymers in which the balance between monomers is shifted.

Here we reveal how intermixing of charged and liganded monomers tunes the cellular uptake and fate of supramolecular polymers and how different ligands can overrule the effects on each other. For this study, bipyridine disc-shaped amphiphiles (discs) were used, which are robust and fluorescent supramolecular monomers that self-assemble into one-dimensional columnar polymers and allow for high density display of ligands. These supramolecular building blocks can be made to interact with biological matter on the level of nucleotides,^[25] proteins^[26] as well as whole cells.^[27] A variety of supramolecular copolymers with different compositions was generated by simple mixing of monomers with diverse properties (Figure 1). The uptake kinetics and valency dependence for supramolecular homopolymers based on amine-, guanidine-, or RGD-functionalized discs were compared using microscopy and cell cytometry, revealing very distinct kinetics and cellular fate. These

[a] S. van Dun, J. Schill, Dr. L.-G. Milroy, Prof. Dr. L. Brunsveld
Laboratory of Chemical Biology, Department of Biomedical Engineering
and Institute for Complex Molecular Systems
Eindhoven University of Technology
Den Dolech 2, 5612 AZ Eindhoven (The Netherlands)
E-mail: l.brunsveld@tue.nl

Supporting information and the ORCID identification number(s) for the author(s) of this article can be found under:
<https://doi.org/10.1002/chem.201804045>.

© 2018 The Authors. Published by Wiley-VCH Verlag GmbH & Co. KGaA. This is an open access article under the terms of Creative Commons Attribution NonCommercial License, which permits use, distribution and reproduction in any medium, provided the original work is properly cited and is not used for commercial purposes.

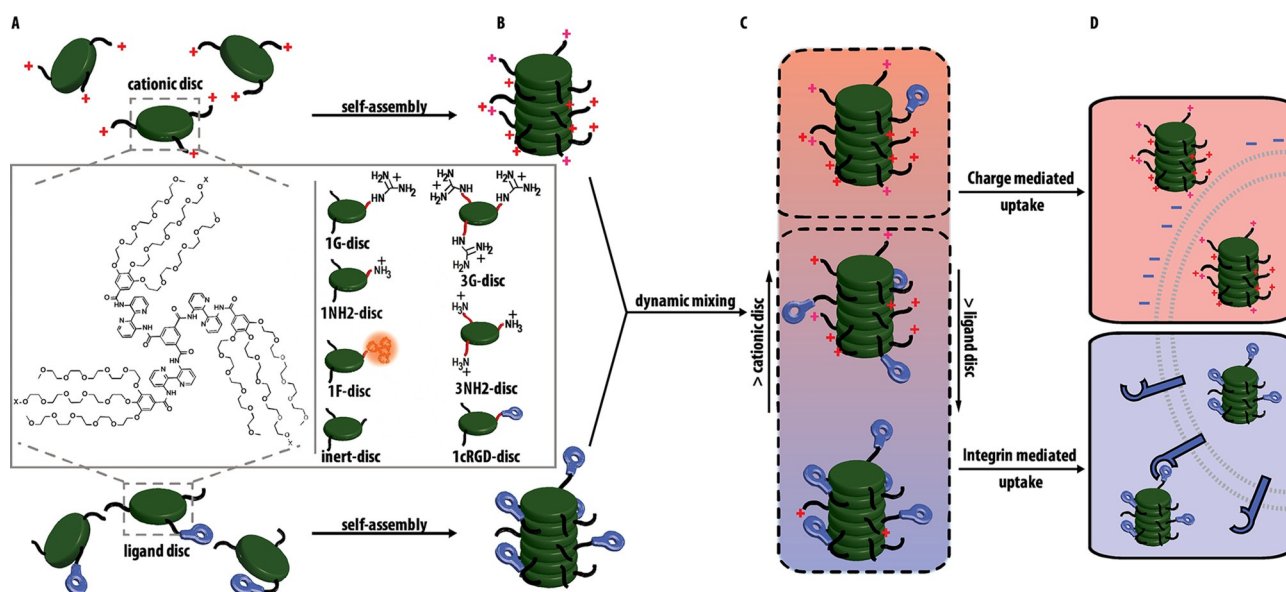


Figure 1. Columnar supramolecular polymers are a modular and controllable platform for interfacing with biological systems. A) Chemical structure of the monomers functionalized with either cationic moieties (amine or guanidine), a ligand (cRGD), or fluorophore (fluorescein). B) Supramolecular homopolymers in water. C) Library of supramolecular copolymers by dynamic mixing of cationic and ligand functionalized monomers. D) Supramolecular copolymers of which the composition determines a mutually exclusive cellular uptake and fate.

distinct characteristics were used to interpret libraries of supramolecular copolymers, revealing mutually exclusive cellular uptake behavior with stringent compositional control by the monomeric building blocks.

Results and Discussion

Synthesis

Supramolecular polymers formed by discs featuring nine peripheral amine groups show cellular uptake and facilitate the uptake of cell-impermeable disc monomers through supramolecular copolymerization.^[28] However, the cellular uptake kinetics of the supramolecular polymers formed by mono- and tri-amino monomers was considered too slow for cellular studies when combined with cell-impermeable monomers. Guanidine moieties have shown optimal properties to disrupt and permeabilize the cellular membrane in comparison to primary amines.^[29] Modification of the disc monomers with guanidine groups was hypothesized therefore to enhance the cellular uptake of the supramolecular polymer. We therefore synthesized mono- and tri-functionalized guanidine disc monomers (**1G-disc**, **3G-disc**) (Figure 1, Scheme S2) by a one-step reaction between 1H-pyrazole-1-carboxamide-hydrochloride and either the one-amine- (**1NH₂-disc**)^[26] or three-amine-disc (**3NH₂-disc**)^[30] to afford the **1G-disc** and **3G-disc** in yields of 80 and 43%, respectively.

Specific, receptor-mediated uptake of supramolecular elements can be achieved by attachment of ligands for these receptors,^[12,23] which we also wanted to recreate in the context of our supramolecular polymers. Therefore, we synthesized a supramolecular monomer functionalized with one cyclic RGD peptide moiety, and one with cyclic RAD as reference, (**1cRGD-**

disc, **1cRAD-disc**) to promote integrin-mediated cellular uptake of the copolymers. Protected cRGD and cRAD peptides were connected via a HBTU-activated amide coupling to the **1NH₂-disc**, which was followed by removal of the protecting groups with TFA, providing the peptide-ligand functionalized disc monomers with yields of 78% and 60% over 2 steps (Scheme S2). Finally, for visualization purposes of the supramolecular polymers via TEM measurements a ferrocene modified disc monomer was prepared. For this, the **1NH₂-disc** was first functionalized with a reactive dibenzocyclooctyne (DBCO) handle via a simple 1 step amide bond formation with *N*-hydroxysuccinimide (NHS)-activated DBCO cross-linker. This was then followed by a copper-free click reaction with azide-ferrocene yielding the **1Fe-disc**.

Self-assembly

The self-assembly of the new peptide and guanidine functionalized discs was first studied with UV/Vis and fluorescence spectroscopy. All new discs showed the typical redshift in the UV/Vis spectrum when dissolved in phosphate-buffered saline (PBS) as well as the characteristic, aggregation-induced, fluorescence intensity increase upon columnar assembly in a polar solvent (Figure S3).^[26,30,31] Single particle tracking (Figure S4) and dynamic light scattering measurements (Figure 2A) confirmed the formation of self-assembled structures as indicated by the scattering correlations of the **1cRGD-disc** and **3G-disc**. TEM measurements were carried out to confirm the columnar geometry of the assembled state. Copolymer of either the **1cRGD-disc** or the **3G-disc** with 10% of the **1Fe-disc** (for scattering purposes), were prepared by simple mixing and visualized using TEM (Figure 2B and Supporting Information Figure S5). Both copolymers formed assemblies of rod-like struc-

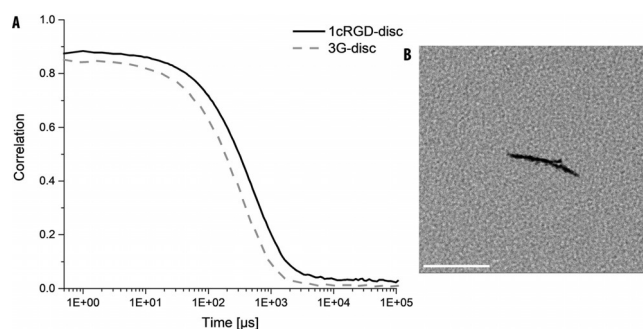


Figure 2. Self-assembly into columnar architectures. A) DLS correlation spectra of **1cRGD-disc** and **3G-disc** in water. B) TEM image of copolymer of **3G-disc** with **1Fe-disc** (9:1). Scale bar represents 50 nm.

ture with a typical length of 50 nm and diameter of around 3 nm, as further testimony to the robustness of the columnar aggregation of these supramolecular discs with diverse side-chain functionalities.

Charge mediated uptake

The cellular uptake properties of supramolecular polymers of different compositions of cationic monomers were compared using live cell imaging. The discs exhibit high fluorescence from the bipyridine central core when polymerized and can be excited using two-photon microscopy.^[28] Supramolecular polymers composed purely of neutral **Inert-disc**, or fluorescein disc (**1F-disc**) (Figure 3A) did not show evidence of cellular uptake, as was the case for supramolecular polymers formed by the single charged **1NH2-disc** and **1G-disc** (Figure S6). By contrast, the triply charged **3NH2-disc** and the **3G-disc** formed homopolymers, which were readily taken up and captured into vesicles as indicated by the observed punctuate distribution (Figure 3A). Therefore, both the amine- and the guanidine-functionalized discs require a charge density of only three cationic groups per monomer for uptake of their corresponding supramolecular polymers. The high density of positive charges present in the supramolecular polymers evidently favors cellular

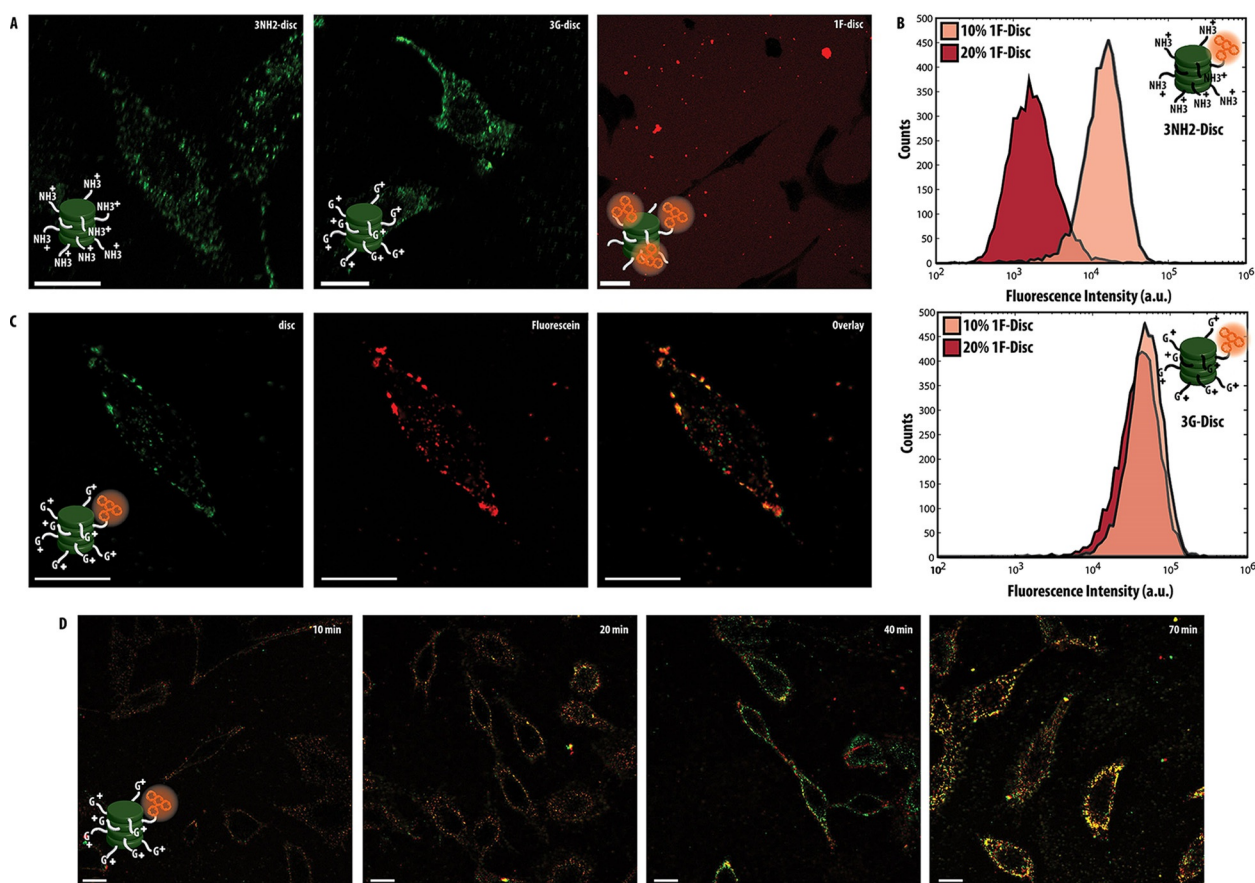


Figure 3. Supramolecular materials with modulated charge type and charge density feature differentiated cellular uptake and cargo co-transport. A) Microscopy images of the cellular uptake of **3NH2-disc**, **3G-disc** or cell impermeable **1F-disc** ($5 \mu\text{M}$) after a 2 h incubation on HeLa cells. The **3NH2-disc**, **3G-disc** (green) were excited at 730 nm with the multi-photon laser while the **1F-disc** (red) was excited 495 nm with the white light laser (WLL). Scale bars represent $25 \mu\text{m}$. B) Flow cytometry analysis of **3NH2-disc** (left) and **3G-disc** (right) copolymers with **1F-disc** (9:1, 8:2, total disc concentration $5 \mu\text{M}$) after 2 h incubation on HeLa cells. C) Microscopy images of the cellular uptake of a **3G-disc:1F-disc** copolymer (ratio 8:2, total disc concentration $5 \mu\text{M}$) after 2 h incubation on HeLa cells. The copolymer was excited at 730 nm with the multi-photon laser to image all the disc (green) and at 495 nm with the WLL to image the **1F-disc** (red). Existence of supramolecular copolymer was represented by the presence of a yellow signal and the absence of free green signal in the overlay image. Scale bars represent $10 \mu\text{m}$. D) Time-lapse (10–70 minutes) of the cellular uptake of **3G-disc:1F-disc** copolymer (ratio 9:1, total disc concentration $5 \mu\text{M}$) by HeLa cells represented by the overlay of the disc and fluorescein channel. Scale bar represent $25 \mu\text{m}$.

uptake but conveniently avoids the need for seven to eight positive charges, typical in covalent systems, and is in line with observations on self-assembling vesicles.^[32,33] The uptake of both these supramolecular polymers was shown to be rather fast as both cationic discs co-localized with the cellular membrane within minutes and internalized after 30 minutes (Figure S7, S8). Incubation of a large cohort of HeLa cells for 16 h, resulted in a more efficient uptake for the **3G-disc** compared to **3NH2-disc** (Figure S9). This increased uptake was also reflected by an increased cytotoxicity of **3G-disc** as verified in an MTT assay (Figure S10). Flow cytometry experiments were performed to quantify the cellular uptake of different supramolecular copolymers containing either **3NH2-disc** or **3G-disc**. For this, 10–20% of **1F-disc** monomer was copolymerized to use the fluorescence of the appended fluorescein as readout for cellular uptake. Our results show that supramolecular polymers copolymerized with **3G-disc** outperformed those with **3NH2-disc** in terms of both the amount of copolymer that is taken up and the efficiency with which otherwise impermeable discs are taken up as copolymers. After 2 h incubation, an almost 8-fold increase in cellular uptake was observed for **3G-disc** copolymerized with 10% **1F-disc**, compared to corresponding **3NH2-disc** copolymer (Figure 3B). An increase in the amount of cell impermeable **1F-disc** (20%) monomer into the supramolecular copolymers resulted in a further 8-fold decrease in uptake for the **3NH2-disc** copolymers. By contrast, the **3G-disc** copolymers featured only a minor decrease in uptake with increasing amounts of **1F-disc**. In line with this, no cellular uptake of the **3NH2-disc**-based copolymers was observed by multi-photon microscopy (Figure S11), whereas the **3G-disc**-based copolymers displayed strong overlapping fluorescence in both the disc and the fluorescein channel (Figure 3C). A time lapse of the **3G-disc:1F-disc** copolymer (Figures 3D and S12) showed a similar uptake profile as for the **3NH2-disc** and **3G-disc** homopolymers (Figures S7 and S8). The cellular internalization only appears to be slightly less progressive as a result of the incorporation of the **1F-disc**. The guanidine moieties in the **3G-disc** thus not only increase the uptake of the resulting supramolecular homopolymers but also install uptake efficiency for cell-impermeable monomers, presumably through incorporation of more cell-impermeable monomers within the copolymer without interfering with the charge-mediated uptake induced by the cationic residues. These results demonstrate, again, the necessity for cell-impermeable monomers such as **1F-disc** to assemble within cell-permeable supramolecular copolymers, here using the charge of **3G-disc**, to be taken up into the cells.

Integrin-mediated uptake

Charge-mediated cellular uptake typically lacks cell-type selectivity; by contrast ligand-mediated uptake can be deployed to selectively target cell-type specific receptors. The **1cRGD-disc** was investigated on cell lines with different expression levels of $\alpha_v\beta_3$ integrins to test for a specific integrin-mediated uptake of the supramolecular copolymers (Figure 4A, S15). Only cells with a passage number below 10 were used to ensure close

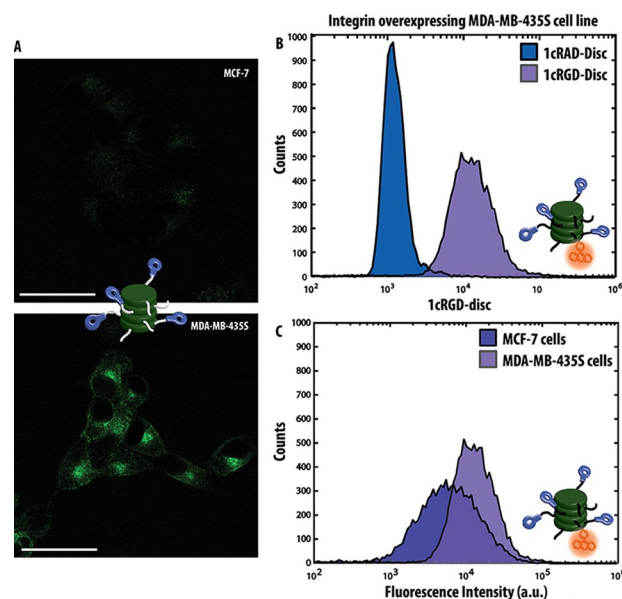


Figure 4. Cell-type specific uptake of supramolecular polymers is modulated via ligand decoration and copolymerization. A) Multiphoton microscopy images of the cellular uptake of **1cRGD-disc** (5 μ M) on MCF-7 and MDA-MB-435S cells, after overnight incubation. Scale bar represents 25 μ m. B) Flow cytometry analysis of **1cRAD-disc** or **1cRGD-disc** copolymers with **1F-disc** (9:1, 5 μ M) after overnight incubation on MDA-MB-435S cells. C) Flow cytometry analysis of **1cRGD-disc** copolymers with **1F-disc** (9:1, 5 μ M) on MCF-7 and MDA-MB-435S cells.

characteristics of the cells to the reference strains. On overnight incubation of a 5 μ M solution of **1cRGD-disc** with the integrin-deficient MCF-7 cell strain, **1cRGD-disc** internalization could hardly be detected. In contrast, upon incubation of the $\alpha_v\beta_3$ integrin-overexpressing cell strain MDA-MB-435S^[34] with **1cRGD-disc** strong uptake was observed and a resulting perinuclear localization for the discs. Incubation of both cell strains with the charged **3G-disc** did not result in a differentiated uptake between the cell lines or any perinuclear localization (Figure S16). To unambiguously identify the role of the integrins in the uptake of the **1cRGD-disc** by the MDA-MB-435S cells, we also evaluated the uptake of the **1cRAD-disc**, which differs from the **1cRGD-disc** by only a single methyl group. The **1cRAD-disc** was not taken up by any of the cell strains tested (Figure S17). This result strongly brings forward the receptor mediated uptake mechanism for the **1cRGD-disc** and simultaneously shows a complete absence of a charge-mediated mechanism for the supramolecular polymers formed by the **1cRGD-disc**.

Studies on mixtures of the **1cRGD-disc** and the **1F-disc** revealed that the **1cRGD-disc** was also capable to enforce the internalization of the otherwise cell-impermeable **1F-disc** via the formation of supramolecular copolymers. Flow cytometry experiments on the integrin rich MDA-MB-435S strain using copolymers of either **1cRGD-disc** or **1RAD-disc** and **1F-disc** (ratio 9:1) clearly showed the dependence of integrin binding on cell uptake through the observation of enhanced uptake by the **1cRGD-disc** copolymer compared to no uptake in the case of the **1cRAD-disc** copolymer (Figure 4B). In line with observa-

tions made for the homopolymers, the time scale of the cellular uptake of the copolymers via the ligand-mediated pathway increased when compared to the charge-mediated uptake (Figure S13, S18), possibly due to saturation of the receptor.^[35] Similar to the homopolymer, the **1 cRGD-disc**-based copolymers with the **1F-disc** exhibited an increased uptake by the MDA-MB-435S strain compared to the MCF-7 strain (Figure 4C).

Dual-molecular targeting

The interplay between the more rapid, but nonspecific, charge-mediated uptake via the **3G-disc** and the specific, but slower, integrin-mediated uptake via the **1 cRGD-disc** was explored via the study of copolymers made from different compositions of the two monomers. The fluorescent **1F-disc** was additionally added enabling flow cytometry analysis, thus effectively yielding supramolecular terpolymers. A clear discrimination in behavior between copolymers of only **1 cRGD-disc** and **1F-disc** and those consisting of only **3G-disc** and **1F-disc** was evident. The charged mediated uptake via the **3G-disc** resulted in a 50-fold increase in cellular uptake (Figure 5). Intriguingly,

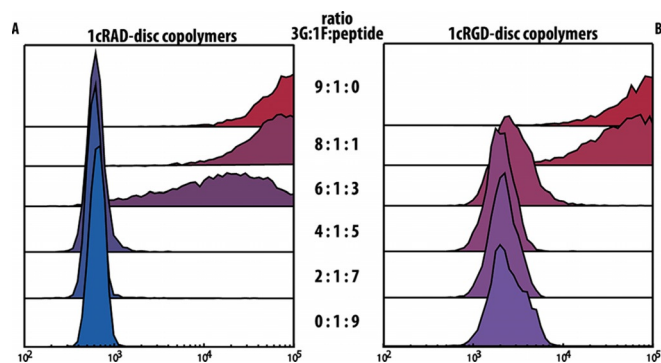


Figure 5. Supramolecular terpolymers reveal cellular uptake mechanisms with sharp compositional transitions. Flow cytometry analysis of a library of terpolymer (5 μM) with a constant amount of **1F-disc** (10%) and different ratios of **3G-disc** and **1 cRAD-disc** (A) or **1 cRGD-disc** (B) after a 7 h incubation with MDA-MB-435S cells.

ingly, terpolymers composed of both **1 cRGD-disc** and **3G-disc** exhibited uptake efficiencies that appear to be governed by either the charge-mediated uptake or the integrin-mediated uptake. These copolymers did not show a well-defined intermediate level of uptake. The terpolymer needed at least 60% **3G-disc** to induce the charge-mediated uptake. By contrast, 30% of the singly functionalized **1 cRGD-disc** already sufficed to favor the integrin-mediated uptake pathway. These observations were not cell-strain dependent as shown by the similar trends observed for the MCF-7 strain (Figure S19). The two cellular uptake mechanisms are thus mutually exclusive for these supramolecular copolymers. This could be a result of the different time scales on which both processes are operating in combination with the need for a minimal concentration of functional groups for the charge-mediated uptake. Supramolecular terpolymers that lacked functional integrin ligands (Figure 5A), required a minimal concentration of charges-in line with other

materials studied^[32,36] for efficient cellular uptake. At least 60% of **3G-disc** was required for uptake of the supramolecular terpolymers comprising the **1 cRAD-disc**. Below this threshold, the terpolymer with the **1 cRAD-disc** was not taken up, as observed for polymers made only from cell-impermeable discs, despite the high similarity with the **1 cRGD-disc** containing terpolymers (Figure S20). The integrin-mediated uptake, though acting slower, required significantly less functional groups in one monomer to enforce the cellular uptake (Figure 5B). The **1 cRGD-disc** features only one ligand per disc, in contrast to the three charges on a **3G-disc**, and can be diluted down to 30%, before the charged mediated uptake takes over.

Conclusion

A modular supramolecular platform for the generation of supramolecular copolymers with tunable cellular uptake capacities was evaluated. Copolymers based on guanidine-functionalized monomers required only three charged groups per monomer and showed improved cellular uptake properties, compared to those featuring amine-functionalized monomers. This improved uptake is accompanied by an increased capacity to deliver cell impermeable monomers via the supramolecular copolymerization. The introduction of a single cRGD peptide per monomer enables uptake of the supramolecular copolymers in a receptor-mediated, cell-specific manner. The modularity of the supramolecular copolymerization concept allowed for the efficient generation of a wide range of terpolymers via the simple co-assembly of different ratios of **3G-disc** and **1 cRGD-disc** with a constant fraction of **1F-disc**. Copolymerization of **3G-disc** with **1 cRGD-disc** results in materials with a mutually exclusive cellular uptake mechanism, in which either the unspecific charge-mediated or the receptor-mediated uptake is dominant. This mutual exclusive cellular uptake, with concomitant sharp compositional transition, provides potential to be further explored for diverse supramolecular material properties. Examples would include activatable cellular uptake platforms, cell selectivity tuning, and cargo delivery, all facilitated by the preparation of these supramolecular copolymers by simple mixing of building blocks.

Experimental Section

Preparation particles

Disc-solutions were prepared by weighing in the disc and dissolving it in PBS (50 μM , cell experiments) or milliQ (100 μM , TEM). Multicomponent polymers were mixed in the proper ratio 2 hours prior use. For cell experiments, polymers were diluted down (5 μM) in DMEM supplemented with 10% FBS and 1% Pen/Strep without phenol red and applied to the cells.

Dynamic light scattering

DLS experiments were performed with the Malvern Zetasizer Nano ZSP. The DLS was equipped with a He-Ne laser operating at 633 nm. Samples (100 μM , milliQ) were filtered (PVDF, 200 μm) prior measurement at 173° at room temperature. Each sample was measured in triplicate (10 \times 10 seconds)

Transmission electron microscopy

Visualization by TEM was performed with a Technai G2 Sphera by FEI operating at an acceleration voltage of 80 kV. Samples were prepared by incubating the target with 10% Fe-disc for visualization at a final concentration of 8.0×10^{-5} M for at least 2 h. Subsequently, 3 μ L of this solution was drop-casted on a 400 square mesh copper grid with a carbon support film and dried for one minute.

Cell culture

MCF-7 and MDA-MB-435S cell lines were cultured in RPMI while 3T3 and Hela cells were cultured in DMEM containing 10% FBS and 1% penicillin/streptomycin. All cells were grown as monolayers in culture flask at 37 °C, 5% CO₂. Cells were passed on when a confluency around 80% was reached. After washing with PBS (3x) the cells were detached by submerging the cells in trypsin for 1 minute at 37 °C, 5% CO₂. Trypsin was deactivated by the addition of 90 vol. % medium. Cell lines were passed at least 3 times before used in confocal or flow cytometry studies and were discarded after passage 10.

Confocal microscopy

Cells were imaged on a Leica TCS SP5X equipped with a HCX PL Apo CS water immersion lens, Leica hybrid detector (HyD) and a temperature controlled incubation chamber (37 °C). MCF-7, 3T3 and MDA-MB435S cells were counted and seeded in 8-well culture slides (20.000 cells per well) using DMEM (3T3) or RPMI1640 (MCF-7 and MDA-MB435S) supplemented with 10% FBS and 1% Pen/Strep. After an overnight incubation at 37 °C, 5% CO₂, the medium was substituted for medium without phenol red containing 5 μ M disc and incubated at 37 °C, 5% CO₂. Prior imaging, the cells were gently washed (2x) with PBS and subsequently imaged right after in medium without phenol red. CYTO59 nuclei life stains were performed according protocol after incubation with disc solutions. Discs were excited with use of the multi-photon laser (730 nm, pin-hole fully open) and detected between 450–600 nm. Fluorescein was excited at 495 nm with the laser and detected between 520–600 nm. CYTO59 was excited at 622 nm with the laser and detected between 640–650 nm.

Flow cytometry

Flow cytometry measurements were carried out on a FACS Aria III (BD Biosciences) equipped with a 70 μ m nozzle. Cells were cultured in a similar fashion as previously described for the confocal microscopy experiments. Also disc-solutions were made in a similar manner. Hela, MCF-7 and MDA-MB-435S cells were harvested via trypsinization for 1 minute at 37 °C, 5% CO₂. Subsequently, the trypsin was inactivated by the addition of 90 vol. % DMEM (Hela) or RPMI1640 (MCF-7 and MDA-MB-435S) supplemented with 10% FBS and 1% Pen/Strep. Cells were counted and seeded in 24 well plates (100.000 cells per well, 450 μ L working volume) and incubated overnight at 37 °C, 5% CO₂. Dependent on the experiment, cells were incubated with 5 μ M disc solutions for a certain period of time, gently washed twice with PBS and trypsinized with 100 μ L trypsin per well for 2 minutes. Trypsin was deactivated by the addition of 90 vol. % medium after which the cells were pelleted by centrifugation for 3 minutes at 3000xg. After drainage of the supernatant, the pellet was resuspended in 200 μ L medium without phenol red but with propidium iodide (PI) (1:200) for 5 minutes before the cell suspension was loaded into the flow cytometer. A

total of 10.000 single cells were counted and afterwards gated based on their forward- vs. side scatter and negative stain for PI to prevent any contribution originating from the uptake of cell permeable apoptotic cells. The fluorescence intensity per cell was measured by exciting the fluorescein on the 1F-disc with a 488 laser and detect through a 530/30 bandpass filter. All samples were measured with a flow rate of 1.0 mL min⁻¹.

Supporting Information

Further details on chemicals, equipment, synthetic procedures, characterization, UV/Vis, fluorescence spectroscopy, nanoparticle tracking analysis, MTT assays, supporting confocal microscopy and flow cytometry data can be found in the supporting information.

Acknowledgements

We would like to acknowledge Katja Petkau-Milroy for providing Inert-disc and amine functionalized disc and Martijn van Rosmalen for help with flow cytometry measurements. This work was funded by The Netherlands Organization for Scientific Research (NWO) via gravity Program 024.001.035, VICI Grant 016.150.366, ECHO Grant 711.013.015, and STW grant 12859-FluNanoPart.

Conflict of interest

The authors declare no conflict of interest.

Keywords: cellular delivery · multicomponent · multivalency · supramolecular chemistry · supramolecular copolymers

- [1] L. Brunsveld, B. J. Folmer, E. W. Meijer, R. P. Sijbesma, *Chem. Rev.* **2001**, *101*, 4071–4098.
- [2] C. D. Jones, J. W. Steed, *Chem. Soc. Rev.* **2016**, *45*, 6546–6596.
- [3] O. J. G. M. Goor, S. I. S. Hendrikse, P. Y. W. Dankers, E. W. Meijer, *Chem. Soc. Rev.* **2017**, *46*, 6621–6637.
- [4] A. Barnard, D. K. Smith, *Angew. Chem. Int. Ed.* **2012**, *51*, 6572–6581; *Angew. Chem.* **2012**, *124*, 6676–6685.
- [5] C. Fasting, C. A. Schalley, M. Weber, O. Seitz, S. Hecht, B. Koksche, J. Drenth, C. Graf, E.-W. Knapp, R. Haag, *Angew. Chem. Int. Ed.* **2012**, *51*, 10472–10498; *Angew. Chem.* **2012**, *124*, 10622–10650.
- [6] M. J. Webber, R. Langer, *Chem. Soc. Rev.* **2017**, *46*, 6600–6620.
- [7] W. T. Al-Jamal, K. Kostarelos, *Acc. Chem. Res.* **2011**, *44*, 1094–1104.
- [8] S. Behzadi, V. Serpooshan, W. Tao, M. A. Hamaly, M. Y. Alkawareek, E. C. Dreaden, D. Brown, A. M. Alkilany, O. C. Farokhzad, M. Mahmoudi, *Chem. Soc. Rev.* **2017**, *46*, 4218–4244.
- [9] K. Petkau-Milroy, L. Brunsveld, *Org. Biomol. Chem.* **2012**, *10*, 219–232.
- [10] B. C. Buddingh, J. C. M. van Hest, *Acc. Chem. Res.* **2017**, *50*, 769–777.
- [11] K. Saha, S. T. Kim, B. Yan, O. R. Miranda, F. S. Alfonso, D. Shlosman, V. M. Rotello, *Small* **2013**, *9*, 300–305.
- [12] J. Brinkmann, E. Cavatorta, S. Sankaran, B. Schmidt, J. van Weerd, P. Jonkheijm, *Chem. Soc. Rev.* **2014**, *43*, 4449–4469.
- [13] G. Gasparini, E.-K. Bang, J. Montenegro, S. Matile, *Chem. Commun.* **2015**, *51*, 10389–10402.
- [14] C.-Y. Jiao, D. Delaroche, F. Burlina, I. D. Alves, G. Chassaing, S. Sagan, *J. Biol. Chem.* **2009**, *284*, 33957–33965.
- [15] Y. A. Nagel, P. S. Raschle, H. Wennemers, *Angew. Chem. Int. Ed.* **2017**, *56*, 122–126; *Angew. Chem.* **2017**, *129*, 128–132.
- [16] L. Fei, L. Ren, J. L. Zaro, W.-C. Shen, *J. Drug Targeting* **2011**, *19*, 675–680.
- [17] C. A. Fromen, T. B. Rahhal, G. R. Robbins, M. P. Kai, T. W. Shen, J. C. Luft, J. M. DeSimone, *Nanomedicine* **2016**, *12*, 677–687.

- [18] K. Koschek, M. Dathe, J. Rademann, *ChemBioChem* **2013**, *14*, 1982–1990.
- [19] M. H. Bakker, R. E. Kiełtyka, L. Albertazzi, P. Y. W. Dankers, *RSC Adv.* **2016**, *6*, 110600–110603.
- [20] M. H. Bakker, C. C. Lee, E. W. Meijer, P. Y. W. Dankers, L. Albertazzi, *ACS Nano* **2016**, *10*, 1845–1852.
- [21] U. Hersel, C. Dahmen, H. Kessler, *Biomaterials* **2003**, *24*, 4385–4415.
- [22] S. Lucie, G. Elisabeth, F. Stéphanie, S. Guy, H. Amandine, A.-R. Corinne, B. Didier, S. Catherine, G. Alexei, D. Pascal, *Mol. Ther.* **2009**, *17*, 837–843.
- [23] J.-H. Seo, S. Kakinoki, Y. Inoue, T. Yamaoka, K. Ishihara, N. Yui, *J. Am. Chem. Soc.* **2013**, *135*, 5513–5516.
- [24] Y. Zhu, J. Feijen, Z. Zhong, *Nano Today* **2018**, *18*, 65–85.
- [25] M. Á. Alemán García, E. Magdalena Estirado, L.-G. Milroy, L. Brunsveld, *Angew. Chem. Int. Ed.* **2018**, *57*, 4976–4980.
- [26] K. Petkau-Milroy, D. A. Uhlenheuer, A. J. H. Spiering, J. A. J. M. Vekemans, L. Brunsveld, *Chem. Sci.* **2013**, *4*, 2886–2891.
- [27] M. K. Müller, L. Brunsveld, *Angew. Chem. Int. Ed.* **2009**, *48*, 2921–2924; *Angew. Chem.* **2009**, *121*, 2965–2968.
- [28] K. Petkau-Milroy, M. H. Sonntag, A. H. A. M. van Onzen, L. Brunsveld, *J. Am. Chem. Soc.* **2012**, *134*, 8086–8089.
- [29] L. Li, I. Vorobyov, T. W. Allen, *J. Phys. Chem. B* **2013**, *117*, 11906–11920.
- [30] M. K. Müller, K. Petkau, L. Brunsveld, *Chem. Commun.* **2011**, *47*, 310–312.
- [31] L. Brunsveld, H. Zhang, M. Glasbeek, J. A. J. M. Vekemans, E. W. Meijer, *J. Am. Chem. Soc.* **2000**, *122*, 6175–6182.
- [32] Y.-R. Yoon, Y. Lim, E. Lee, M. Lee, *Chem. Commun.* **2008**, 1892.
- [33] J. Schill, S. van Dun, M. J. Pouderoijen, H. M. Janssen, L.-G. Milroy, A. P. H. J. Schenning, L. Brunsveld, *Chem. Eur. J.* **2018**, *24*, 7734–7741.
- [34] A. Taherian, X. Li, Y. Liu, T. A. Haas, *BMC Cancer* **2011**, *11*, 293.
- [35] G. Kibria, H. Hatakeyama, N. Ohga, K. Hida, H. Harashima, *J. Controlled Release* **2011**, *153*, 141–148.
- [36] M. Hellmund, K. Achazi, F. Neumann, B. N. S. Thota, N. Ma, R. Haag, *Biomater. Sci.* **2015**, *3*, 1459–1465.

Manuscript received: August 7, 2018

Accepted manuscript online: August 29, 2018

Version of record online: October 11, 2018